Thermodynamic analyzes of film cooling for a restructured cooling holes at the end of gas turbine engine combustor

Ehsan Kianpour, Nor Azwadi Che Sidik, Mohammad Hussein Razavi, Mohammad akbari,

Masoud Afrand, Iman Golshokouh

***Abstract*—**This research was done to analyze the effects of two different blowing ratios of BR=1.25 and BR=3.18 on the film cooling effectiveness at the combustor outlet, whereas the cylindrical and row trench holes with alignment angle of +60 degrees were considered. In the current research, a three-dimensional representation of a Pratt and Whitney gas turbine engine was simulated and analyzed with a commercial finite volume package FLUENT 6.2.26. This study has been carried out with Reynolds-averaged Navier-Stokes turbulence model (RANS) on internal cooling passages. The combustor combines the interaction of two rows of dilution jets, which are staggered in the stream-wise direction and aligned in the span-wise direction, with that of film cooling along the combustor liner walls. The entire findings of the study showed that trenched holes performed much more efficiently at both blowing ratios, especially at BR=3.18.

***Keywords*—**Gas Turbine Engine, Film-Cooling, Cylindrical Cooling Hole, Trenched Cooling Hole,

I. Introduction

GAS turbine industries try for better performance and power to weight ratio. Brayton cycle (Fig. 1) is appropriate for this purpose. In this cycle, to have better gas turbine engine performance, the combustor's outlet temperature or turbine's inlet temperature (T3) must increase [1]. However, the combustor outlet temperature is so high that no material can resist against this temperature and hence all are finally melted [2]. Furthermore, the combustor outlet temperature increment extends an extremely harsh environment for critical downstream components. Accordingly, a cooling method need be used to pull up the critical parts thermal degradation. A common way currently used is film cooling whose effectiveness is improved by increasing the blowing ratio. In this technique, a thin low temperature boundary layer is developed by cooling holes and is attached on the protected surface.

To improve film cooling effectiveness, the blowing ratio must

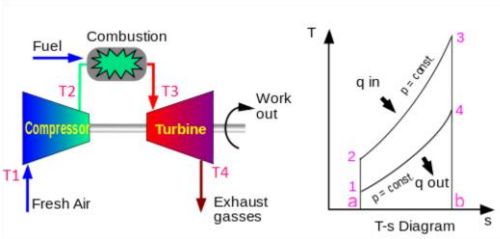

Fig. 1 Schematic view of idealized Brayton cycle

be increased. However, achieving a better attachment of coolant on the surface especially at higher blowing ratios is required. Using trenching cooling holes, researchers can modify the flow behavior and the thermal characteristics. In the trenched cooling holes, the injected coolant is suddenly spread before exiting the cooling holes and entering the main flow. As a result, the film cooling effectiveness is enhanced [3]. Azzi and Jurban [4] tested several ways to study the film cooling thermal field. In this study, they used standard k-ε turbulence model to solve the Reynolds averaged Navier-Stokes equation. In concurred with Rozatiand Danesh Tafti [5], results show that the film cooling effectiveness was improved at low blowing ratios. Kianpour et al. [6,7] in 2012, simulated the combustor end wall cooling holes with two different layouts and exit section area. The results declared that while, the central part of the jets stayed nominally at the same temperature level for both configurations, the temperatures adjacent the wall and between the jets was a while cooler with less cooling holes. Aga and Abhari [8], I-Chien, Yun-Chung, Pei- Pei and Ping-Hei [9] studied the effects of different inclination and lateral angles of holes on film cooling performance. The finding indicated that averaged adiabatic film cooling effectiveness was two times more than stream wise injection at high compound angles especially at high blowing ratios. Sundaram and Thole [10] and Lawson and Thole [11] studied the effects of trenched depth and width on film cooling performance at the vane end wall. The results

E. K. Department of Mechanical Engineering, Najaf Abad Branch, Islamic Azad University, Isfahan, Iran, (corresponding author to provide phone: +98-(31)4229-2881; e-mail: ekianpour@gmail.com).

C. S. N. A. Faculty of Mechanical Engineering, Universiti Teknologi Malaysia, Johor Bahru, Malaysia, (e-mail: azwadi@fkm.utm.my).

M. H. R. Department of Mechanical Engineering, Najaf Abad Branch, Islamic Azad University, Isfahan, Iran, (e-mail: rdehkordi@gmail.com).

M. A. Department of Mechanical Engineering, Najaf Abad Branch, Islamic Azad University, Isfahan, Iran, (e-mail: m.akbari.g80@gmail.com).

M. A. Department of Mechanical Engineering, Najaf Abad Branch, Islamic Azad University, Isfahan, Iran, (e-mail: masoud_afrand@yahoo.com).

I. G. Department of Mechanical Engineering, Izeh Branch, Islamic Azad University, Khoozestan, Iran, (e-mail: golshokooh@yahoo.com).

showed that the maximum cooling effectiveness is obtained at the trench depth of 0.80D. However, Lawson and Thole stated that the trench depth of 0.8D has negative effect on the cooling performance downstream the cooling hole. Yiping et al. [3] tested the effects of depth and width of trenches on the film cooling under overall cooling effectiveness of ϕ=0.6. Also it is figured out that the third (w=2.0D and d=0.75D) and fourth(w=3.0D and d=0.75D) case were more effective than other cases and base line case and it means the trench depth of 0.75D was the optimum one as well as approved by CFD studies. It appears from the last studies that a variety of investigation have been conducted for the effects of cooling hole arrangement, however, only attempt was made to analyze the effect of trenching cooling holes adjacent the combustor end wall surface. This leads to some unanswered questions: How trenched cooling holes improve the film-cooling effectiveness at the combustor end wall surface compared to cylindrical holes? How do cylindrical and trenched cooling holes perform at different blowing ratios? Therefore, the purpose of this research was to analyze the film-cooling effectiveness variation with different arrangements of cooling holes and blowing ratios. Also, in order to determine the validity of the findings, a comparison between the data attained from this investigation and Vakil and Thole [1] and Stitzel and Thole [12] projects was carried out.

II. Research Methodology

In this study, a three-dimensional representation of a true Pratt and Whitney gas turbine engine was simulated and analyzed to get fundamental data. The schematic view of the combustor is shown in Fig. 2.

The width, inlet height and the length of the combustor was 111.8 cm, 99.1 cm and 156.9 cm respectively. The contraction angle was 15.8 degrees that began at x=79.8 cm. The inlet

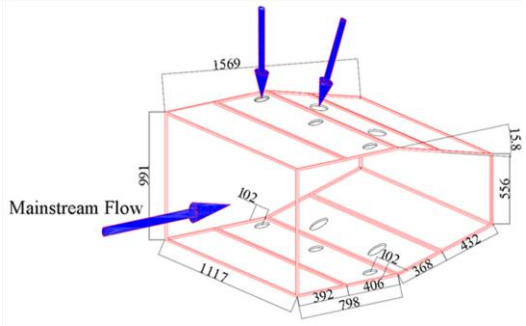

Fig. 2 Schematic view of the combustor simulator (a) top view (b) side view (all dimensions are in cm)

cross sectional area was 1.11m^2 and the exit cross-sectional area was 0.62m^2 . The combustor simulator included four film-cooled stream wise panels. The starting point of these panels was approximately at 1.6m upstream of the turbine vanes. These panels were 39.2, 40.6, 36.8 and 43.2 centimeter in length respectively. The low thermal conductivity of combustor panels were 1.27 cm in thickness, which allowed for adiabatic surface temperature measurements. Two different rows of dilution holes were considered within the second and third panels. These dilution rows were located at 0.67m and 0.90m downstream of the beginning of the combustor liner panels. The diameter of the first row of dilution holes was 8.5 cm and for the second row, it was 11.9 cm. The center line of the second row was staggered with respect to the first row of dilution holes. To verify the purpose of this study, a three-dimensional representation of a Pratt and Whitney gas turbine engine was simulated. The present combustor simulator included two configurations of cooling holes. The first

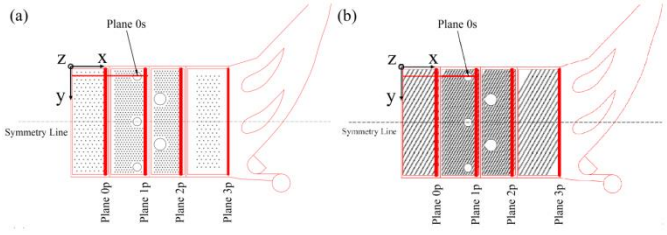

Fig. 3 Location of the measurement planes (a) baseline (b) Case 2

arrangement (baseline) was designed similar to Vakil and Thole [1]. For both cases, the film cooling holes were positioned in equilateral triangles. The diameter of the film cooling holes was 0.76 cm and drilled at an angle of 30 degrees from the horizontal surface. The length of film cooling holes in the baseline case was 2.5 cm. For the next case (Case 2), the cooling holes were located within a row trench with alignment angle of +60 degrees. Furthermore, the trench depth and width were 0.75D and 1.0D, respectively. The purpose of the current research was to analyze the effects of cooling holes restructure on the film cooling performance through a combustor simulator at two coolant blowing ratios of BR=1.25 and BR=3.18. The thermal distribution within a combustor simulator was measured along the specific measurement planes (Fig. 3).

In order to attain precisely analyzing and reasonable time consumption, about 8×10^6 tetrahedral meshes were used as adopted in the study by Stitzel and Thole [13]. According to the specific flow ratio at the inlet of volume control, inlet mass flow boundary condition was defined. Wall boundary condition and slipless boundary condition were applied to limit the interaction zone between fluid and solid layer. The pressure outlet boundary condition was used at the end of control volume. In addition, both cases were completely symmetrical along the x-y and x-z planes. According to this issue, symmetry boundary condition $\partial/\partial n$=0 was as applied. To analyze the flow behavior through the control volume, the governing equations were used.

momentum equation

$$\frac{\partial}{\partial t}\left(\rho u_i\right)+\frac{\partial}{\partial x_j}=\left(\rho u_i u_j\right)=-\frac{\partial P}{\partial x_i}+\frac{\partial \tau_{ij}}{\partial x_i}+\rho g_i+\vec{F}_i \qquad (1)$$

the continuity equation

$$\frac{\partial \rho}{\partial t}+\frac{\partial}{\partial x}\frac{dx}{dt}+\frac{\partial \rho}{\partial y}\frac{dy}{dt}+\frac{\partial \rho}{\partial z}\frac{dz}{dt}=-\rho(\nabla.V) \quad (2)$$

and the energy and RNG *k-ε* equations

$$\frac{\partial}{\partial t}(\rho E)+\frac{\partial}{\partial x_i}\left(u_i(\rho E+P)\right)= \frac{\partial}{\partial x_i}\left(k_{eff}\frac{\partial T}{\partial x_i}-\sum_j h_j J_j+u_j(\tau_{ij})_{erf}\right)+S_h \quad (3)$$

$$\frac{\partial}{\partial t}(\rho k)+\frac{\partial}{\partial x_i}(\rho k u_i)=\frac{\partial}{\partial x_j}\left(\left(\mu+\frac{\mu_t}{\sigma_k}\right)\frac{\partial k}{\partial x_j}\right)+P_k-\rho\varepsilon \quad (4)$$

$$\frac{\partial}{\partial t}(\rho \varepsilon)+\frac{\partial}{\partial x_i}(\rho \varepsilon u_i)=\frac{\partial}{\partial x_j}\left(\left(\mu+\frac{\mu_t}{\sigma_\varepsilon}\right)\frac{\partial \varepsilon}{\partial x_j}\right) +C_{1\varepsilon}\frac{\varepsilon}{k}P_k-C^*_{2\varepsilon}\rho\frac{\varepsilon^2}{k} \quad (5)$$

The first-order upwind and central differencing scheme were used to approximate the convective and diffusion terms in the differential equation, respectively. To check the convergence, the mass residue of each control volume has been calculated and the maximum value has been used to check for the convergence. The convergence criterion has been set to 10^{-4}. To understand the thermal field results, the quantities should be defined. Film cooling effectiveness is defined as below:

$$\eta=\frac{T-T_\infty}{T_C-T_\infty} \quad (6)$$

In the equation above, T is the local temperature, T_∞ is the main stream temperature, and T_C is the temperature of coolant.

III. Findings and Discussion

Fig. 4 illustrates the fluctuations of film cooling observed in the current study as well as the experimental findings and the CFD prediction by Stitzel and Thole [26].

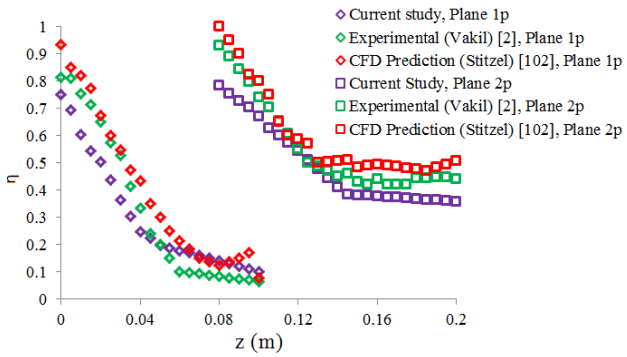

Fig. 4 The film cooling effectiveness comparison of planes 1p and 2p along y/W=0.4

The results gained from the computations done by means of FLUENT software were compared to the experimental data related to film cooling effectiveness that Stitzel and Thole [13] and Vakil and Thole [1] had collected in their separate studies. The data was extracted for planes 1p and 2p. The operating conditions of the investigations were exactly the same so that the comparison would be reasonably adequate and practical.

The plot clarify that for plane 1p, different solutions are satisfactorily consistent. However, it appears that a good prediction can be made based on the present study because the value gained in this analysis is closer to the CFD prediction data for z=4.5cm. Within measurement plane of 2p, Vakil's model and Stitzel's CFD prediction possess reasonable consistency, the lowest performance could be seen in the present study. The investigation was under-predicted and this was intensified adjacent the combustor end wall surface (z=1cm). Also, the variation between the current study computation and benchmarks were calculated as follows:

$$\%Diff=\frac{\sum_{i=1}^{n}\frac{x_i-x_{i,benchmark}}{x_{i,benchmark}}}{n}\times 100 \quad (7)$$

The deviation of film cooling effectiveness from experimental data gathered by Vakil and Thole [1] and CFD prediction by Stitzel and Thole [26] was equal to 11.14% and 15.79% and 6.35% and 11.14% for measurement planes of 1p and 2p, respectively.

Fig. 5 shows the variations of film cooling effectiveness for different measurement planes and mass flux ratios of BR=1.25 and BR=3.18 at y=30cm and along z axis.

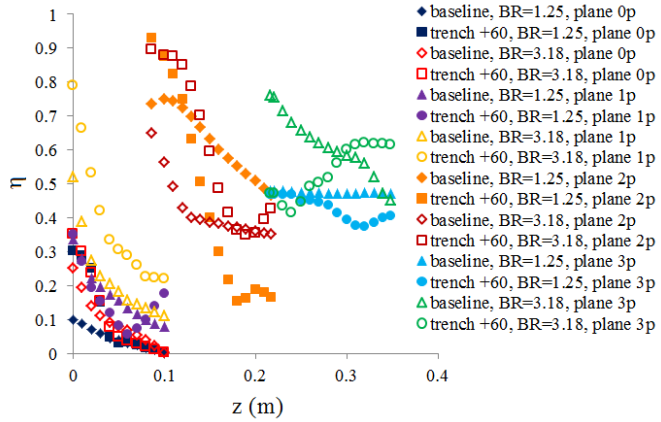

Fig. 5 The changes of film cooling effectiveness for different configurations

For the measurement plane of 0p and at low blowing ratio of BR=1.25, the trenched holes with the alignment angle of +60 degrees performed the most effectively adjacent to the end wall surface. Film cooling effectiveness increases up to 200% as compared to the cylindrical case. But for the next two measurement planes and at the same blowing ratio, film cooling effectiveness increased only 4% and 26.4% respectively. As can be seen, at a low blowing ratio of BR=1.25, the cooling effectiveness is similar for both the

baseline and the trenched holes with an alignment angle of +60 degrees which is about η=0.475. At higher blowing ratio, the film exiting the trenches created a new boundary and enhanced heat transfer coefficients significantly downstream of the trench.

Film cooling effectiveness in plane 1p was taken directly downstream of the first row of the dilution jets. This particular hole is centrally located right at the mid pitch within the combustor simulator. The results of the thermal field are shown in Fig. 6. The center of the dilution jet is reasonably centered about the corners of this observation plane as the dilution jet surges up. Note that jet spreading there is slightly higher for y=10cm and y=50cm. This may be due to the jet's interaction with its top row.

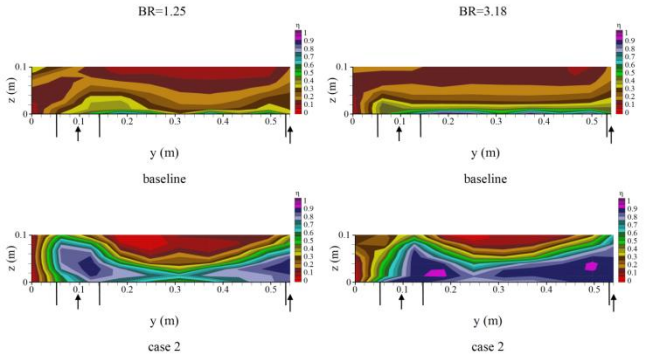

Fig. 6 Film-cooling effectiveness distribution of plane 1p

Also, contrary to the baseline, it is slightly hotter (0<η<0.05) for the trenched case with alignment angle of +60 degrees in the position of 14cm<y<52cm and 8cm<z<10cm. However, compared to other cases, this type of trenched holes, adjacent to end wall surfaces, perform more efficiently. For BR=3.18, note that when film-cooling significantly increased, the dilution jet injection remained the same. Also this figure shows slightly higher levels near the wall for the trenched cases relative to the baseline, especially for the trenched holes with alignment angle of +60 degrees. However, no major improvements in cooling were observed along the liner wall. It was just downstream of the dilution jet and near the corners that the thermal field contours indicated that the film-cooling were being entrained by the upward motion of the dilution jet. Moreover, the temperature was slightly higher (0<η<0.05) for the trenched holes with alignment angle of +60 degrees at the position of 18cm<y<28cm and 38cm<y<50cm. For trenched holes with alignment angle of +60 degrees, the area was visible over the range of 14cm<y<52cm and 8cm<z<10cm at blowing ratio of BR=1.25.

Fig. 7 shows the contours of film cooling effectiveness in plane 2p at both BR=1.25 and BR=3.18 located one dilution hole diameter (1D2) downstream of the trailing edge of a dilution two hole. The plane covers almost half pitch of the combustor simulator and shows the second rows of dilution in reasonable detail. As can be seen on the right of the figure, the mushroom shaped temperature profiles got mixed and a warmer region near the mid-span emerged. There is a probability that the warm region is formed as a result of the flow of unmixed warmer fluid around the stagnation region caused by the impact of opposing dilution jets in the first row. The high temperature region observed along y=52cm and height of z=15cm was the footprint of the warm fluid trapped in the recirculating region downstream of the first row of dilution jets. This region was warmer for the trenched holes row with alignment angle of +60 degrees (0<η<0.05). At the midspan, the remnants of trapped fluid behind the first row dilution jet show core temperatures ranging between 0<η<0.05 for the row trenched cooling holes with alignment angle of +60 degrees. At BR=3.18, the injection of coolant into the mainstream is the basic difference between the obtained contours. Right at the trailing edge of the second row of dilution jets and at higher blowing ratios, the trenched holes created a protective layer (10cm<y<50cm) on the critical surfaces which was more efficient than that of the baseline. This was especially remarkable for the trenched holes with alignment angle of +60 degrees (0.9<η<1.0). While the highest film cooling layer at low blowing ratio BR=1.25 reached at z=14cm at the mid pitch (which was 14% of the combustor inlet height) at BR=3.18, this layer reached at z=18cm for the trenched holes with alignment angle of +60 degrees.

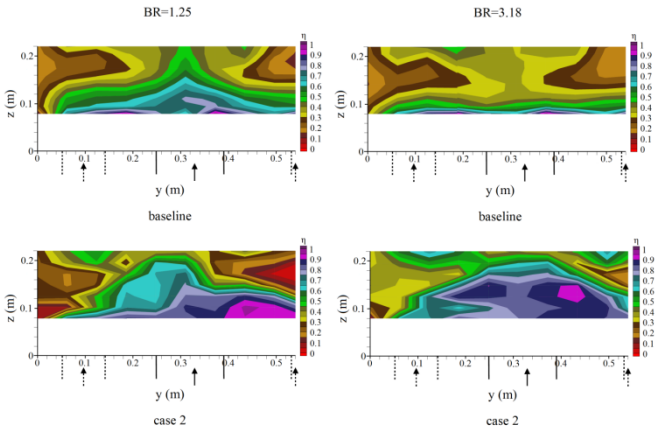

Fig. 7 Film-cooling effectiveness variation of plane 2p

Fig. 8 illustrates the profile of a stream-wise temperature through the first row of dilution jet that covered a length of second cooling panel and was centered at x/L=0.43 and y/W=0.1.

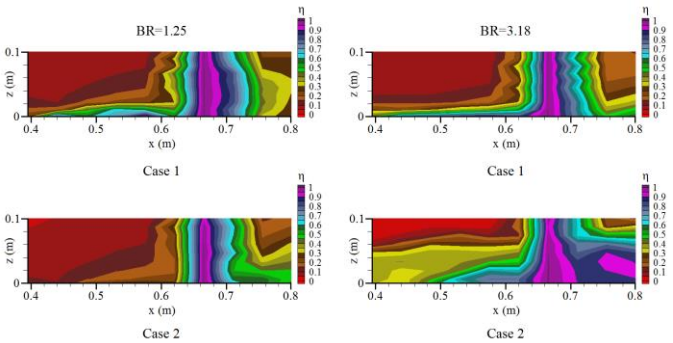

Fig. 8 Film-cooling effectiveness variation for plane 3p

The coolest core of dilution jet can be seen between 64.3cm<x<70.6cm as it enters into the mainstream. Just downstream of the dilution jet, the layer of low temperature region (η=0.3) reached to z=2 cm for the trenched holes with the alignment angle of +60 degrees. However, the high temperature region downstream of the first row of dilution jet reached to η=0.05 for the trenched holes with the alignment angle of +60 degrees. Interesting was the film cooling interaction with the dilution jet itself. At the leading edge of the dilution jet, a relatively thick layer of film-coolant stagnated onto the dilution jet and carried away by the dilution jet.

The shear forces at the trailing edge of the jet took advantage of the stagnated flow by entraining it, and consequently created the entrainment or recirculating region behind the dilution jet. Besides these observations, temperature gradients at the jet mainstream interface were quite large at the leading edge of the dilution jet. At the trailing edge of the jet, thermal contours could be seen to spread as a result of turbulent mixing induced by the dilution flow. Furthermore, the entrainment of the film-cooling at the trailing edge of the dilution hole was clearly visible around the centerline of the dilution jet. However, the entrainment effects would become weaker with the increase of distance from the core of the jet, especially in the case of the trenched holes with the alignment angle of +60 degrees. At BR=3.18, the temperature contours immediately behind the jet show a thinner layer of film cooling when the flow is entrained into the jet. As the entrainment effects became less strong further away from the jet, the flow reversed and the vectors seemed to follow along the temperature contours, which were growing thicker due to the enhanced turbulence behind the dilution jet. Much of the film-coolant was entrained and carried away by the dilution jet right at the trailing edge, thus leaving behind a thinner film of coolant. This entrainment, or recirculating region behind the dilution jet, could also be seen within observation plane of 0s.

IV. Conclusion and Recommendation

The purpose of this study was to highlight the effects of two different blowing ratios of BR=1.25 and BR=3.18 on the film-cooling performance with two configurations of cooling holes, cylindrical and row trenched holes with alignment angle of +60, near the combustor simulator endwall surface. In this research, a three-dimensional representation of a true Pratt and Whitney gas turbine engine was analyzed with a commercial finite volume package Fluent 6.2.26. As a summary for all schemes, the film-cooling layer is growing at higher BR; it was thinned by the application of cylindrical holes for plane 2p. In addition, the central part of the plane 2p showed severe penetration of the cooling jets and a thick film-cooling layer creation for the trenched form. On the other hand, blowing ratio increase led to a cooler region near the wall and between the jets, particularly for the trenched cases. The thermal field findings depicted a recirculation area extended at just downstream of the jet where the entrainment of film cooling was occurred by the dilution jet. The streamwise thermal field contours indicated a strong effect of trenched cooling holes and dilution injection downstream the dilution jet, especially for the trenched holes and high blowing ratios. For the measurement plane of 0p, 1p and for all schemes, the film-cooling effectiveness enhancement occurred with blowing ratio increase. While, for the plane 2p, the film-cooling effectiveness reduced with blowing ratio enhancement. Based on the results of the current study, there are several recommendations to notice. Since the dimension of aero-engines is different with the geometry of the current case of study and these types of engines operate at different altitudes and the surrounding conditions affect the efficiency of the engine, it is recommended to study the effects of trenched cooling holes at the combustor end wall surface of these engines at a variety range of operating altitudes.

References

[1] S. S. Vakil, K. A. Thole, "Flow and Thermal Field Measurements in a Combustor Simulator Relevant to a Gas Turbine Aero engine." Journal of Engineering for Gas Turbines and Power, vol. 127, 2005, pp. 257 - 267.

[2] W. Colban, K. A. Thole, M. Haendler, "Experimental and Computational Comparisons of Fan-Shaped Film Cooling on a Turbine Vane Surface." Journal of Turbomachinery, vol. 129, 2007, pp. 23-31.

[3] L. Yiping, A. Dhungel, S. V. Ekkad, R. S. Bunker, "Effect of Trench Width and Depth on Film Cooling From Cylindrical Holes Embedded in Trenches." Journal of Turbomachinery, vol. 131, 2009, pp. 011003-1-011003-13.

[4] A. Azzi, B. A. Jubran, "Influence of leading edge lateral injection angles on the film cooling effectiveness of a gas turbine blade," Journal of Heat and Mass Transfer, vol. 40, 2004, pp. 501–508.

[5] A. Rozati, K. Danesh Tafti, "effect of coolant–mainstream blowing ratio on leading edge film cooling flow and heat transfer – LES investigation," Journal of Heat and Fluid Flow, vol. 29, 2008, pp. 857–873.

[6] E. Kianpour, C. S. Nor Azwadi, M. Agha Seyyed Mirza Bozorg, "Thermodynamic analysis of flow field at the end of combustor simulator." International Journal of Heat and Mass Transfer, vol. 61, 2013, pp. 389–396.

[7] E. Kianpour, C. S. Nor Azwadi, M. Agha Seyyed Mirza Bozorg, "Dynamic analysis of flow field at the end of combustor simulator." Jurnal Teknologi, vol. 58, 2012, pp. 5–12.

[8] V. Aga, R. S. Abhari, "Influence of Flow Structure on Compound Angled Film Cooling Effectiveness and Heat Transfer." Journal of Turbomachinery, vol. 133, 2011, pp. 031029-1-031029-12.

[9] L. I-Chien, C. Yun-Chung, D. Pei-Pei, C. Ping-Hei, "Film Cooling Over a Concave Surface through Two Staggered Rows of Compound Angle Holes." Journal of Chinese Institute of Engineers, vol. 28, 2005, pp. 827-836.

[10] N. Sundaram, K. A. Thole, "Bump and Trench Modifications to Film-Cooling Holes at the Vane-End wall Junction." Journal of Turbomachinery, vol. 130, 2008, pp. 041013-1-041013-9.

[11] S. A. Lawson, K. A. Thole, "Simulations of Multiphase Particle Deposition on End wall Film-Cooling Holes in Transverse Trenches." Journal of Turbomachinery, vol. 134, 2012, pp. 051040-1- 051040-10.

[12] S. Stitzel, K. A. Thole, "Flow Field Computations of Combustor-Turbine Interactions Relevant to a Gas Turbine Engine." Journal of Turbomachinery, vol. 126, 2004, pp. 122-129.